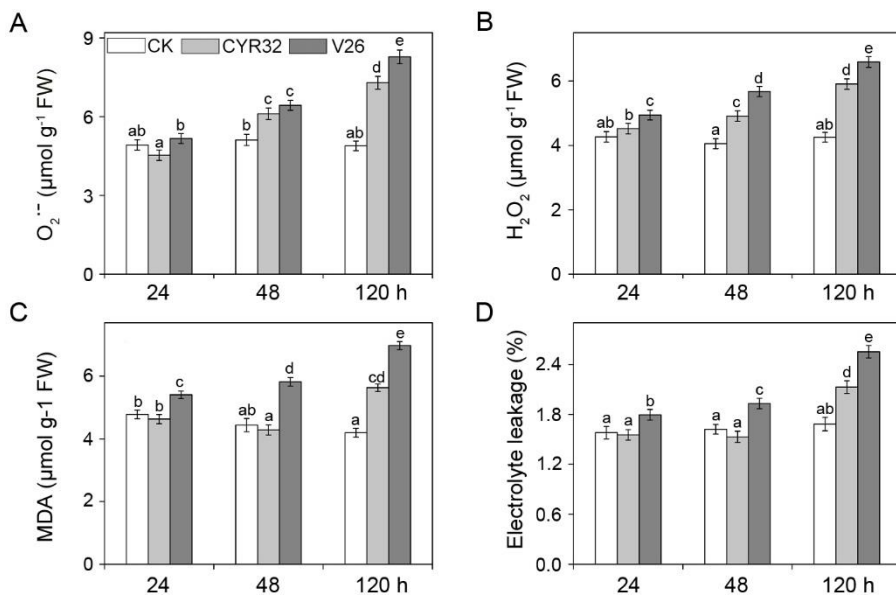
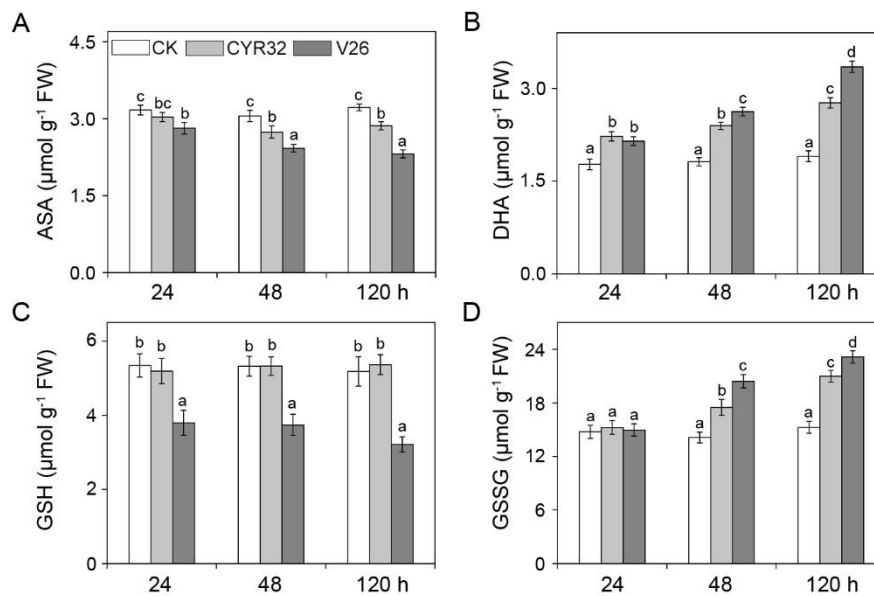


**Figure S1.** Chlorophyll content (A), total protein content (B), soluble sugar (C), and proline (D) in wheat cultivar CM42 inoculated with CYR32 and V26. Bars represent standard deviations (SD) which were calculated from four independent biological replicates ( $n = 4$ ). Different letters note significant differences among different treatments ( $P < 0.05$ ) following Duncan's multiplication range test. CK, un-inoculated wheat plants. 24-120 hpi represent 24, 48, and 120 h post-inoculation.



**Figure S2.** Superoxide anion radicals ( $O_2^{\bullet-}$ ) production rate (A), hydrogen peroxide ( $H_2O_2$ ) content (B), the malondialdehyde (MDA) content (C), and electrolyte leakage (D) in wheat cultivar CM42

inoculated with CYR32 and V26. Bars represent standard deviations (SD) which were calculated from four independent biological replicates ( $n = 4$ ). Different letters note significant differences among different treatments ( $P < 0.05$ ) following Duncan's multiplication range test. CK, un-inoculated wheat plants. 24-120 hpi represent 24, 48, and 120 h post-inoculation.



**Figure S3.** The concentrations of antioxidants in wheat cultivar CM42 inoculated with CYR32 and V26. AsA, ascorbic acid (A); DHA, dehydroascorbic acid (B); GSH, reduced glutathione (C); GSSG, oxidized glutathione (D). Bars represent standard deviations (SD) which were calculated from four independent biological replicates ( $n = 4$ ). Different letters note significant differences among different treatments ( $P < 0.05$ ) following Duncan's multiplication range test. CK, un-inoculated wheat plants. 24-120 hpi represent 24, 48, and 120 h post-inoculation.

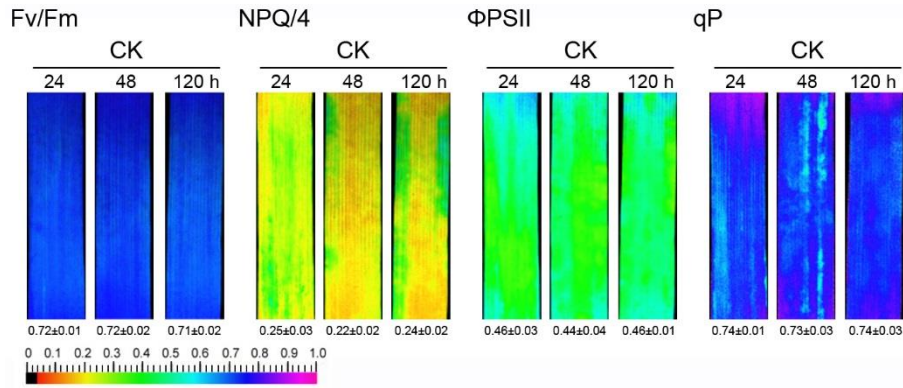


**Figure S4.** Chlorophyll fluorescence parameters ( $F_v/F_m$ , maximum efficiency of PSII photochemistry; NPQ, non-photochemical quenching;  $\Phi_{PSII}$ , quantum yield of PSII electron transport; qP, photochemical quenching) in the un-inoculated wheat plants at 24, 48, and 120 hpi. Quantitative values ( $\pm$  SD) are shown below each fluorescence images. CK, un-inoculated wheat plants.

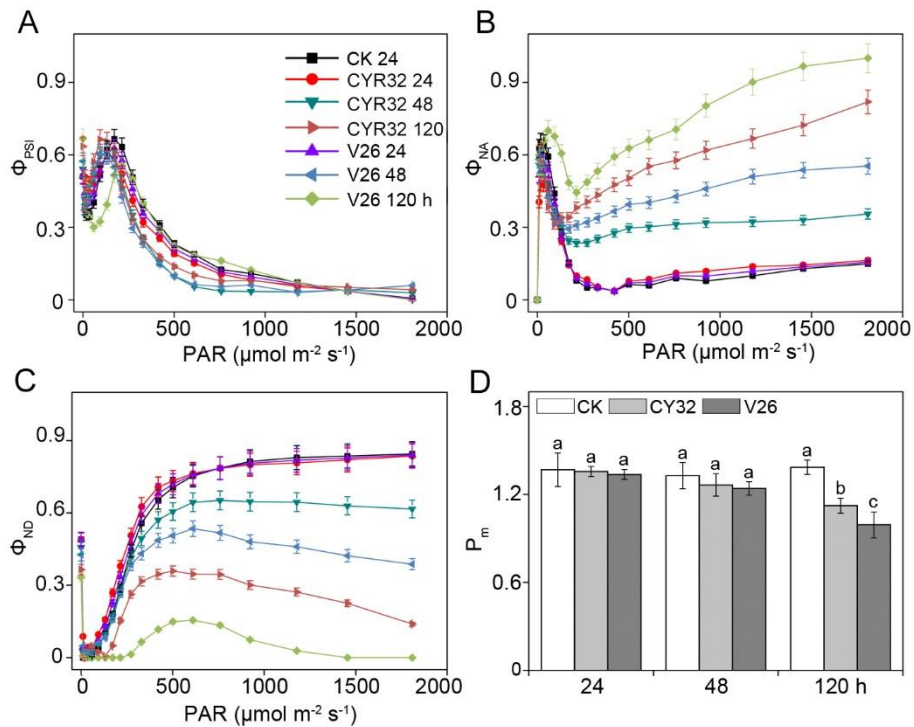


**Figure S5.** The values of parameters derived from P700 absorbance in wheat cultivar CM42 inoculated with CYR32 and V26.  $\Phi_{PSI}$  (A), effective quantum yield of photosystem I;  $\Phi_{NA}$  (B), quantum yield of non-photochemical energy dissipation of PSI reaction centers due to acceptor side

limitation;  $\Phi_{ND}$  (C), quantum yield of nonphotochemical energy dissipation in PSI reaction centers due to donor side limitation;  $P_m$  (D), maximal P700 signal. Bars represent standard deviations (SD) which were calculated from four independent biological replicates ( $n = 4$ ). Different letters note significant differences among different treatments ( $P < 0.05$ ) following Duncan's multiplication range test. CK, un-inoculated wheat plants. 24-120 hpi represent 24, 48, and 120 h post-inoculation.

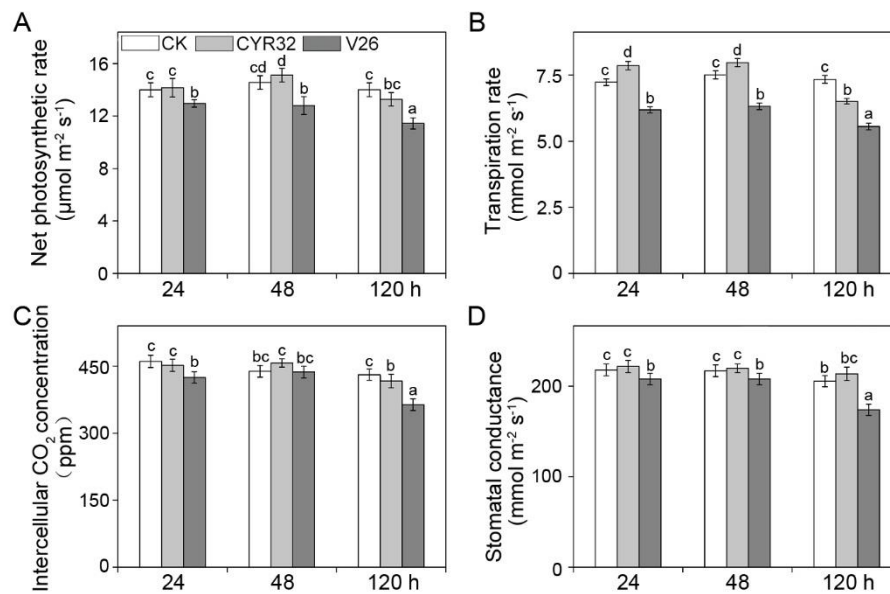


**Figure S6.** Net photosynthetic rate (A), transpiration rate (B), intercellular CO<sub>2</sub> concentration (C), and stomatal conductance (D) in wheat cultivar CM42 inoculated with CYR32 and V26. Bars represent standard deviations (SD) which were calculated from four independent biological replicates ( $n = 4$ ). Different letters note significant differences among different treatments ( $P < 0.05$ ) following Duncan's multiplication range test. CK, un-inoculated wheat plants. 24-120 hpi represent 24, 48, and 120 h post-inoculation.